Agricultural Water Management, 8 (1984) 119—131
Elsevier Science Publishers B.V., Amsterdam — Printed in The Netherlands

THE USES AND LIMITATIONS OF FLUX-GRADIENT RELATIONSHIPS IN MICROMETEOROLOGY

M.R. Raupach[1] and B.J. Legg[2]

1 *Division of Environmental Mechanics, CSIRO, P.O. Box 821, Canberra City, A.C.T. 2601 (Australia)*
2 *Physics Department, Rothamsted Experimental Station, Harpenden, Herts. (Great Britain)*

ABSTRACT

This paper presents some new wind-tunnel observations on flux-gradient relationships for momentum and heat just above a slightly heated rough surface, with emphasis on the implications for evapotranspiration measurement. The dimensional arguments leading to the concept of a flux-gradient relationship are shown to be valid only within a limited region, the inertial sublayer, which is separated from the surface by a roughness sublayer in which the dimensional arguments no longer apply. The wind-tunnel results show that the observed turbulent diffusivity for heat in the roughness sublayer is greater than the value expected from inertial-sublayer theory by a factor γ_H which is about 2 near the surface and exceeds 1 throughout a layer of depth of about 10 h (h being the roughness element height). No such enhancement is seen for momentum.

INTRODUCTION

Vertical fluxes of water vapour, heat, momentum and trace constituents are commonly measured in the atmospheric surface layer by several micrometeorological techniques, including eddy correlation, profile, Bowen ratio and bulk aerodynamic methods. Except for eddy correlation, all these are based on assumptions about relationships between vertical fluxes and vertical gradients. For momentum, heat and water vapour, for example, the flux-gradient relationships take the familiar forms:

$$\overline{u'w'} = -\tau/\rho = -K_M \partial\tilde{u}/\partial z \ , \qquad (1)$$

$$\overline{w'\theta'} = H/(\rho c_p) = -K_H \partial\tilde{\theta}/\partial z \ , \qquad (2)$$

$$\overline{w'q'} = E/\rho = -K_E \partial\tilde{q}/\partial z \ , \qquad (3)$$

where u is the streamwise and w the vertical wind component, θ potential temperature, q specific humidity, τ Reynolds shear stress, H sensible heat flux, E water vapour flux, ρ air density, c_p specific heat of air at constant

0378-3774/84/$03.00 © 1984 Elsevier Science Publishers B.V.

pressure, z height, and K_M, K_H and K_E are turbulent diffusivities for momentum, heat and water vapour, respectively. Overbars denote time averages and primes departures therefrom.

The flux-gradient relationships are fixed by specifying the turbulent diffusivities $K_{M,H,E}$. Different flux-measuring techniques require different degrees of specification: for example, the profile method requires complete determination of $K_{M,H,E}$, whereas the Bowen ratio method for measuring water vapour or heat fluxes requires only the assumption $K_H = K_E$ (Thom, 1975). Whatever assumption is involved, it is clearly important in crop micrometeorology to have reliable knowledge about flux-gradient relationships, and their limitations, for the flow above plant canopies and roughness arrays in general.

This paper presents some wind-tunnel observations on flux-gradient relationships for momentum and heat just above a rough surface. The implications for evapotranspiration measurement of these observations, and of related field data, are discussed. As a preliminary, the arguments leading to Eqns. (1), (2) and (3) are briefly recalled from a slightly wider viewpoint than usual.

GRADIENT-DIFFUSION THEORIES IN BOUNDARY LAYERS

Gradient-Diffusion Theories and Their Limitations

Consider a transported species S, such as momentum heat or water vapour, with concentration s (per unit volume of air) and vertical flux density F_S. A turbulent diffusivity K_S for this species may be defined by the relationship:

$$F_S = \overline{w's'} = -K_S \partial\bar{s}/\partial z \qquad (4)$$

which involves only the local turbulent flux and the local mean gradient in the same (vertical) direction. Although K_S always exists in a mathematical sense, it generally depends both on past history of the flow and on the behaviour of the flow in a region surrounding the point of interest; in other words, it is a non-local property of the turbulent velocity field. However, if K_S at a particular point is assumed to depend only on known geometrical properties such as the height of the point, and on simple mean local flow properties such as $\overline{u'w'}$ or $\partial\bar{u}/\partial z$ at that same point, then Eqn. (4) becomes a simple gradient-diffusion model of turbulent transport. Flux-gradient relationships are examples of such models.

It is well known (Corrsin, 1974) that gradient-diffusion models can only be justified when the length scale of the turbulence is much smaller than the length scale over which mean gradients change appreciably. In inhomogeneous turbulence, which includes almost all turbulent flows in nature, these two length scales are of the same order (Tennekes and Lumley, 1972). Hence, there are no general grounds for believing that K_S can be specified in the way required to construct a useful gradient-diffusion model. Indeed, there are several cases where Eqn. (4) can only be satisfied with a negative K_S. For example, Bradley et al. (1983) found that this occurred for vertical heat and water vapour transport within a forest canopy. The implied counter-gradient transport is evidence for the failure of gradient diffusion models in situations where their underlying assumptions no longer hold.

In spite of the lack of a general justification, gradient-diffusion models are still useful in limited circumstances. If the only external parameters controlling the turbulent velocity and concentration statistics are a single length scale $\underline{L}$, a single velocity scale $\underline{U}$ and a single concentration scale $\underline{S}$, then any turbulence statistic must be expressible as a dimensionally consistent function of only $\underline{L}$, $\underline{U}$ and $\underline{S}$. For K_S, this implies:

$$K_S/(\underline{U}\ \underline{L}) = \text{constant} \tag{5}$$

where the dimensionless constant is the same throughout the flow region controlled only by $\underline{U}$ and $\underline{L}$ (if this were not so, some other external parameter would have to be involved). However, the constant is not necessarily the same for different species S, such as momentum and heat.

We now consider which regions in the atmospheric boundary layer are sufficiently restricted in their controlling parameters for Eqn. (5) to be applied.

Boundary-Layer Structure

A well-developed turbulent boundary layer consists of an outer layer and a surface layer (usually the inner 15% or so of the overall boundary layer) in which vertical fluxes do not vary significantly with height. Considering only the neutral surface layer for the moment, a controlling velocity scale is provided by the friction velocity $u_* = (\tau/\rho)^{\frac{1}{2}}$, which scales the constant momentum flux. Possible length scales are the effective height z-d (d being the zero-plane displacement of the rough surface) and surface scales such as the roughness-element height h, breadth ℓ, separation D, and perhaps others. It is necessary to define d, which has often been regarded as no more than a fitting parameter in the logarithmic mean wind profile

$$\bar{u}(z) = \frac{u_*}{k} \ln \left[\frac{z-d}{z_o}\right] \quad , \tag{6}$$

where $k(\cong 0.4)$ is the von Karman constant and z_o the roughness length of the surface. Thom (1971) suggested that d is the mean height of momentum absorption by the rough surface. This physical definition was supported recently by Jackson (1981), who argued that just as the velocity scale u_* is set by the amount of momentum absorbed by the surface, so the length scale z-d is determined by the mean height of that absorption.

Provided that the effective height z-d is large compared with the length scale h, ℓ, D of the surface roughness, these surface-defined scales are not dynamically significant and the only scales remaining to control the flow are u_* and z-d itself. Hence, Eqn. (5) is applicable, showing that $K_S \propto u_*(z-d)$. The region where this is true is called the inertial sublayer (Tennekes and Lumley, 1972; p. 146). At smaller heights the length scales of the surface roughness become dynamically significant and no simple dimensional conclusion can be made about K_S. This lower region is called the roughness sublayer (Fig. 1).

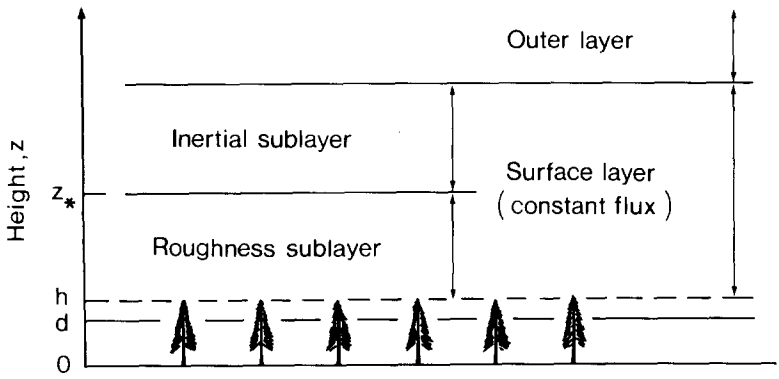

Fig. 1. The surface layer and its sublayers.

In non-neutral conditions, the extension of this dimensional analysis is the Monin-Obukhov similarity theory (Monin and Yaglom, 1971; Chpt. 4). The end result for K_S is the same except that the "constant" in Eqn. (5) is a function of a single dimensionless stability parameter, conventionally taken as

$$\xi = \frac{z-d}{L} = \frac{-kg\,\overline{w'\theta'}(z-d)}{T_o\,u_*^3} \tag{7}$$

where L is the Monin-Obukhov length, k($\cong$ 0.4) the von Karman constant, g gravitational acceleration and T_o a reference absolute temperature. The dimensional requirement for inertial-sublayer flow is now

$$K_S = K_S^*(\xi) = ku_*(z-d)/\phi_S^*(\xi) \quad , \tag{8}$$

where $\phi_S^*(\xi)$ is an influence function which must be determined empirically. Star superscripts denote diffusivities and influence functions applicable in the inertial sublayer only. For momentum, heat and water vapour, the functions $\phi_S^*(\xi)$ are experimentally defined fairly well in unstable conditions ($\xi < 0$) and less well defined in unstable conditions ($\xi < 0$), the consensus for neutral conditions ($\xi = 0$) being that

$$1 = \phi_M^*(0) = \phi_H^*(0) = \phi_E^*(0) \tag{9}$$

(Dyer, 1974; Yaglom, 1977; Bradley et al., 1981a,b). Note that $\phi_M^*(0) = 1$ is required so the Eqns. (8) and (1) give the logarithmic wind profile, Eqn. (6), in the inertial sublayer.

In the roughness sublayer, dimensional analysis does not lead to simple results because the effects of roughness geometry are dynamically significant. An observed characteristic of this layer is that the turbulent diffusivity K_S tends to be greater than the value K_S^* expected from the inertial-sublayer prediction, Eqn. (8). A convenient descriptor of this enhancement is the ratio

$$\gamma_S = K_S/K_S^* \quad , \tag{10}$$

which is unity in the inertial sublayer and greater than unity in the roughness sublayer. The upper height limit z_{*S} of the region where $\gamma_s \neq 1$ is also an important property, as it determines where the simple turbulent diffusivity, Eqn. (8), can be applied.

A WIND-TUNNEL EXPERIMENT ON TURBULENT DIFFUSIVITIES IN THE SURFACE LAYER

We now describe a wind-tunnel experiment in which measurements were obtained of γ_S and z_{*S} for momentum and heat in a near-neutral boundary layer over a typical rough surface. The heat was supplied from a plane source close to the top of the roughness elements, thus simulating the daytime situation in a plant canopy. The data presented here were obtained during a recent series of experiments on the turbulent dispersion of trace heat in a simulated atmospheric surface layer (Raupach and Legg, 1983).

Experimental Details

Figure 2 shows the experimental layout in the Pye Laboratory wind-tunnel (CSIRO Division of Environmental Mechanics, Canberra), the working section of which is 11 m long, 1.8 m wide and 0.65 m high. The experimental rough surface was densely-packed 7 mm road gravel, glued to baseboards. With the aid of an upstream trip, this surface generated a deep, near-equilibrium turbulent boundary layer in which the maximum wind speed was about 11 m s^{-1}. Except near the sides of the tunnel, the flow was homogeneous in the lateral direction.

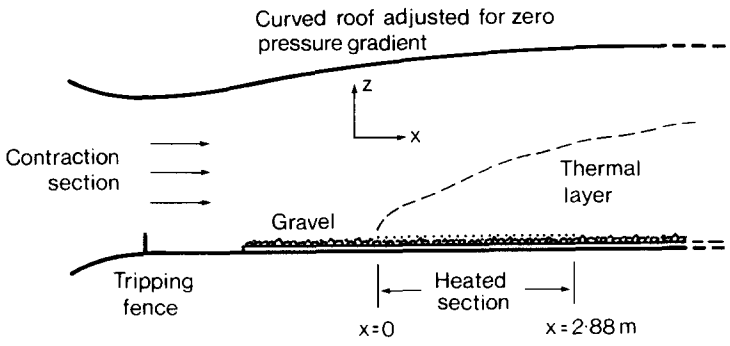

Fig. 2. Experimental arrangement in the wind-tunnel, with vertical axis not to scale.

Part of the rough surface was made into a plane heat source by running wires laterally over the gravel, with a spacing of 2 cm between wires. The wires rested on the gravel and provided an effective plane heat source of strength $H_o \cong 200$ W m^{-2}, nearly spanning the tunnel width and extending 2.88 m in the streamwise direction. Careful checks showed that almost all the heat supplied electrically to the heating wires was transferred to the air, the losses by conduction through the floor (1.4%) and radiation (5.5%) being small and subsequently removed by subtraction to give an accurate measure of H_o as (electrical power) - (losses).

The instantaneous wind components u and w, were measured with an X-wire anemometer, and the temperature θ with a fine-wire (1.2 μm) resistance thermometer; these sensors being positioned close together on a traversing mechanism. The data were digitized on-line at 2.5 kHz, enabling turbulent fluxes and other statistics to be subsequently calculated.

Wind and Temperature Statistics

Figure 3 shows some wind statistics in vertical profile (the height z being measured from an origin, z = 0, at the baseboard surface) at two streamwise stations (x = 0.96 m and x = 2.88 m, where x = 0 is the start of the heated section). The mean wind $\bar{u}$ at both stations obeys the logarithmic wind profile, Eqn. (6), when d is 6 mm, and implies a roughness length z_o of about 0.15 mm. The kinematic Reynolds stress $\tau/\rho = -\overline{u'w'}$ is constant with height up to z ≅ 150 mm, giving a measured friction velocity $u_* = 0.50$ m s^{-1} and a measured von Karman constant k of 0.37 (estimated error ± 0.02), from Eqn. (6). This is perfectly acceptable, given the continuing controversy about the value of k. The standard deviations of u and w, σ_u and σ_w, also have measured values which are consistent with known atmospheric surface layer behaviour. None of the wind statistics vary significantly in the streamwise direction. All of this shows, and other statistics not presented here confirm, that the wind-tunnel boundary layer is a good representation of the near-neutral atmospheric surface layer.

Figure 4 shows some properties of the thermal layer at each station. The mean temperature $\bar{\theta}$ (relative to the upstream air temperature, θ = 0), and the standard deviation of temperature σ_θ, both have vertical profiles which grow with increasing x as the heated layer deepens, roughly as $x^{0.8}$. An important consistency check on the measurements of $\bar{u}$, $\bar{\theta}$ and H_o is provided by the integrated heat conservation equation:

$$H_o x = \rho c_p \int_o^\infty (\bar{u}\,\bar{\theta} + \overline{u'\theta'})\, dz \,, \qquad (11)$$

which state that the heat power $H_o x$ put into the thermal layer upstream of x must pass as an integrated flux through a vertical plane at x. Direct checks of Eqn. (11) at several stations, from x = 0.48 m to x = 2.88 m, show that the left- and right-hand-sides always agree to within 5%. The contribution of the turbulent streamwise flux $\rho c_p \overline{u'\theta'}$ to the right-hand-side of Eqn. (11) is about $-0.1\, xH_o$, decreasing slightly with increasing x; thus, the turbulence transports heat upstream against the dominant advective heat flux $\rho c_p \bar{u}\bar{\theta}$.

The vertical heat flux $\rho c_p \overline{w'\theta'}$ was measured in two ways: firstly from the w and θ signals as an eddy covariance (shown as points in Fig. 4), and secondly from the conservation equation for mean temperature, which is for a

$$\bar{u}\frac{\partial\bar{\theta}}{\partial x} + \frac{\partial\overline{u'\theta'}}{\partial x} + \frac{\partial\overline{w'\theta'}}{\partial z} = 0 \qquad (12)$$

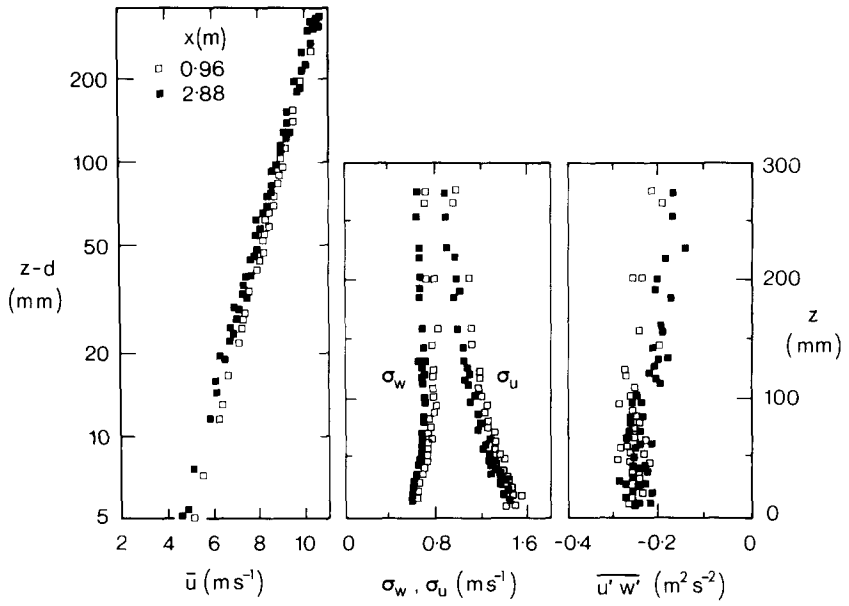

Fig. 3. Vertical profiles of mean wind speed $\bar{u}$ (logarithmic height axis), standard deviations σ_u and σ_w, and kinematic stress $\overline{u'w'}$ (linear height axes) at x = 0.96 m and x = 2.88 m.

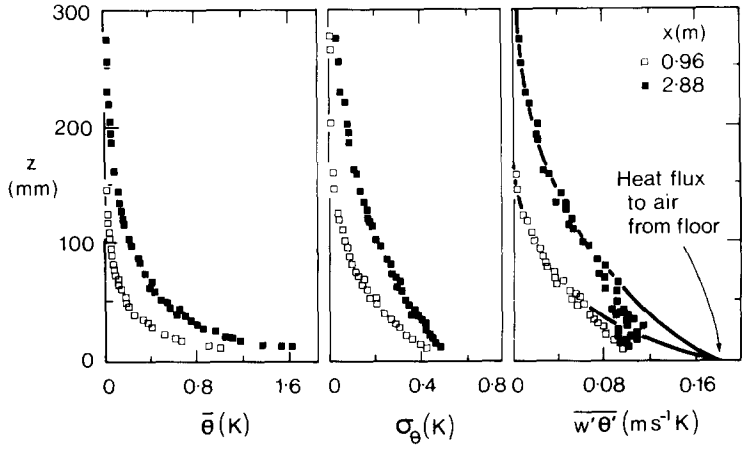

Fig. 4. Vertical profiles through the thermal layer of mean temperature $\bar{\theta}$, standard deviation of temperature σ_θ, and vertical heat flux $h/(\rho c_p) = \overline{w'\theta'}$ (points: covariance; curves: heat budget) at x = 0.96 m and x = 2.88 m.

stationary, two-dimensional flow. By integrating measured values of the first two terms in Eqn. (12) over z, with the lower boundary condition $\overline{w'\theta'} = H_o/\rho c_p$, we obtain the heat flux profiles shown as curves in Fig. 4. These are probably accurate to within ±10% over the bulk of the profile but are more accurate close to the ground, where H_o provides an accurately known point. The two methods agree well when $z \gtrsim 60$ mm, but below this level the eddy covariance systematically underestimates $\overline{w'\theta'}$ because of a combination of high frequency loss and loss due to the separation of the wind and temperature sensors. Spectral analyses confirmed that the underestimation is due to these causes, and also verified that $\overline{u'w'}$ is not significantly in error.

Within the thermal layer, buoyancy was negligible and the heat acted as a passive additive. At z-d = 100 mm, Eqn. (7) shows that $\xi = (z-d)/L = -0.001$, a value so close to zero that the boundary layer can be assumed neutral with confidence.

Turbulent Diffusivities for Momentum and Heat

The turbulent diffusivities

$$K_M = \frac{-\overline{u'w'}}{(\partial\bar{u}/\partial z)} \quad , \qquad K_H = \frac{-\overline{w'\theta'}}{(\partial\bar{\theta}/\partial z)} \tag{13}$$

were calculated, at a number of heights within the thermal layer, from local measured flux values (for heat, using values from temperature conservation equation) and local gradient values obtained from parabolic fits to small segments of $\bar{u}$ and $\bar{\theta}$ profiles. These diffusivities were expressed as ratios γ_M and γ_H to the inertial sublayer forms $K_M^* = K_H^* = ku_*(z-d)$, as in Eqn. (10). The measured wind-tunnel values of k (=0.37) and u_* (=0.50 m s^{-1}) were used.

Figure 5 shows the results for γ_M and γ_H at four stations from x = 1.44 m to x = 2.88 m. Since γ_M is close to 1 throughout the range of measurement, there is no discernible layer of enhanced diffusivity for momentum. The depth z_{*M} of any such layer must obey $z_{*M}-d < 5$ mm. However, for heat, γ_H is 2 near the surface and decreases to 1 throughout a layer whose depth is given by $z_{*H}-d \cong 70$ mm. In terms of surface scales, this is 10 h or $500z_o$. The behaviour of γ_H does not depend in any obvious way upon streamwise position. There is evidently a substantial layer of enhanced diffusivity for heat.

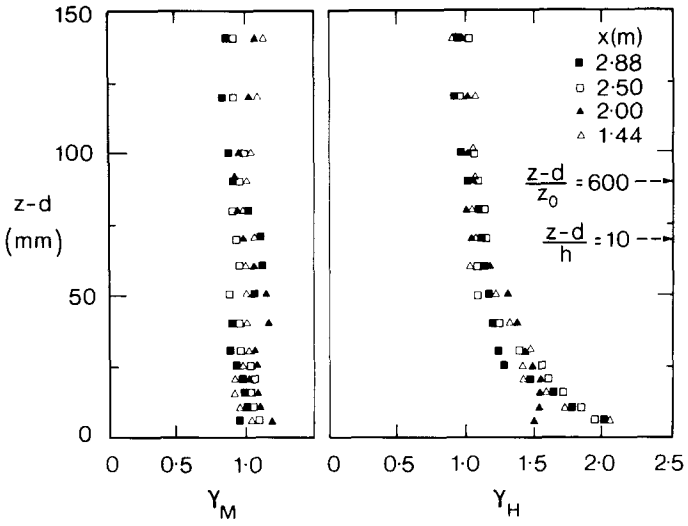

Fig. 5. Enhancement factors γ_M and γ_H at four stations, plotted against height. Height scales in terms of h and z_o are indicated on right.

DISCUSSION

Experimental Limitations

There is no near-surface layer of constant heat flux in this experiment (Fig. 4), in contrast with the substantial constant-flux layer for momentum (Fig. 3). The absence of a constant-flux layer for heat is consistent with the presence of a significant advection term $\bar{u}\partial\bar{\theta}/\partial x$ in Eqn. (12), as suggested by the $\bar{\theta}$ profiles in Fig. 4. In the context of wind-tunnel studies on developing thermal layers within turbulent boundary layers, this is not a surprising result. Similar behaviour has been observed for thermal layers over smooth walls (Antonia et al., 1977), and has been predicted theoretically with the assumption that the thermal layer is approximately self-preserving (Townsend, 1965a,b). These considerations, together with our confidence in the value of H_o (which is supported by Eqn. (11)) lead us to believe that the divergent heat fluxes found from the temperature conservation equation, and represented by the curves in Fig. 4, are correct. Accordingly, the γ_H values in Fig. 5 are based on these fluxes.

The presence of flux divergence raises the possibility that the departure of γ_H from unity close to the surface is caused by flux divergence rather than by rough-surface influence. Two pieces of evidence suggest, however, that flux divergence is not the dominant influence on γ_H. Firstly, similar

studies on thermal layers over slightly heated smooth walls (Orlando et al., 1974; Antonia et al., 1977) show no systematic departure of γ_H from unity near the surface even though heat flux divergence and temperature advection were just as marked in the smooth-wall experiments as in the present, rough-wall case. (Note that the smooth-wall results are expressed in terms of the turbulent Prandtl number $Pr = K_M/K_H$. In neutral conditions $Pr = \gamma_H^{-1}$, from Eqns. (8) to (10)).

Secondly, an experiment on the dispersion of heat from a transverse elevated line source (Raupach and Legg, 1983) has been carried out in the same turbulent flow as used in the present work. The source height was $z-d = 60$ mm. For an elevated source, simple gradient-diffusion theory is expected to apply only in the "far-field" part of the plume (here, $x > 0.5$ m where the source is at $x = 0$); in the "near-field", turbulence memory effects reduce the effective turbulent diffusivity below its far-field value. Calculations of γ_H in the far-field part of the plume gave results similar to those in Fig. 5, with $\gamma_H = 1$ over the bulk of the plume, but $\gamma_H > 1$ close to the surface ($z-d \lesssim 50$ mm). However, the scatter was greater than in Fig. 5 because of the greater complexity of the $\bar{\theta}$ and $\overline{w'\theta'}$ profiles. This comparison suggests that the behaviour of γ_H in Fig. 5 is independent of the specific source geometry, and in particular would still be observed for ground sources extending to large distances upwind. Further wind-tunnel experimental work on this question is desirable.

Comparison with Atmospheric Results

The enhancement of γ_H near the surface is in accord with several atmospheric results which have found that $\gamma_H \cong 2$ close above forests and savannah (Garratt, 1978; Raupach, 1979; Raupach and Thom, 1981; Bradley et al., 1983). In the present experiment, enhancement of K_H occurs over a surprisingly large effective depth, $z_{*H}-d$, of about 10 h or 500 z_o. This is about twice the depth inferred by Garratt (1980) by upward extrapolation of measured λ_H values over savannah, although Garratt's result must depend on the form he assumed for the height dependence of γ_H. It is conceivable that the behaviour of K_H found here is typical of all atmospheric surfaces, as the experimental evidence for the "accepted" formula, $K_H = ku_*(z-d)$, in neutral conditions comes entirely from surfaces with very small roughness-to-measurement height ratios.

There is no reason to restrict this conclusion to heat. In the experiment reported here, the heat was passive and acted simply as a tracer so that any other passive scalar would have behaved identically if released from the same source. This implied, in particular, that $K_H = K_E$, a suggestion

confirmed by limited observations over forests which give $\gamma_H \cong \gamma_E \cong 2$ (Raupach, 1979; Bradley et al., 1983). Hence, provided the source-sink distributions for heat and water vapour are similar, as they are over most closed canopies, the Bowen-ratio method for measuring E should be reliable even though the height of observation is usually well within the roughness sublayer.

For momentum, the situation is not as clear because previous results are not easily reconciled. The present result, that $z_{*M}-d < h$, is broadly consistent with previous wind tunnel work, which found little or no enhancement of K_M close to a variety of surfaces (O'Loughlin and Annambhotla, 1969; Mulhearn and Finnigan, 1978; Raupach et al., 1980). However, field results from a savannah surface with widely separated elements (Garratt, 1980) suggested that z_{*M} increases with element separation D.

In general, gradient-diffusion theories and the associated flux-gradient relationships become progressively less reliable as one approaches a rough vegetated surface until they fail entirely within the canopy, where negative turbulent diffusivities are observed (Bradley et al., 1983). Considerable effort is being made to find physically-based, reliable models for vertical turbulent transport in these situations. Among the promising avenues are higher-order closure methods, Markov-chain simulations of scalar dispersion by a known wind field, and "clean-sweep" models in which the large, coherent motions responsible for much of the transport are modelled separately from the small-scale diffusion.

ACKNOWLEDGEMENTS

B.J. Legg wishes to thank the Agricultural Research Council, U.K., the Royal Society, London, and the CSIRO, Australia, for financial support during the period of this work. Mr. O.A. Simakoff assisted in the construction of the rough surface and heat source. We thank Mr. E.K. Webb for his careful criticism of the manuscript.

REFERENCES

Antonia, R.A., Danh, H.Q. and Prahbu, A., 1977. Response of a turbulent boundary layer to a step change in surface heat flux. J. Fluid Mech., 80: 153-177.

Bradley, E.F., Antonia, R.A. and Chambers, A.J., 1981a. Turbulence Reynolds number and the turbulent kinetic energy balance in the atmospheric surface layer. Boundary-Layer Meteorol., 21: 143-197.

Bradley, E.F., Antonia, R.A. and Chambers, A.J., 1981b. Temperature structure in the atmospheric boundary layer I. The budget of temperature variance. Boundary-Layer Meteorol., 20: 275-292.

Bradley, E.F., Denmead, O.T. and Thurtell, A.W., 1983. Measurements of the turbulence and heat and moisture transport in a forest canopy. Q.J.R. Meteorol. Soc. (in preparation).

Corrsin, S., 1974. Limitations of gradient transport models in random walks in turbulence. Adv. Geophys., 18A: 25-60.

Dyer, A.J., 1974. A review of flux-profile relationships. Boundary-Layer Meteorol., 7: 363-372.

Garratt, J.R., 1978. Flux profile relations above tall vegetation. Q.J.R. Meteorol. Soc., 104: 199-212.

Garratt, J.R., 1978. Surface influence upon vertical profiles in the atmospheric near-surface layer. Q.J.R. Meteorol. Soc., 106: 803-819.

Jackson, P.S., 1981. On the displacement height in the logarithmic velocity profile. J. Fluid Mech., 111: 15-25.

Monin, A.S. and Yaglom, A.M., 1971. Statistical Fluid Mechanics: Mechanics of Turbulence, Vol. 1 (Editor Eng. Trans. J.L. Lumley). M.I.T. Press, Cambridge, Mass., U.S.A.

Mulhearn, P.J. and Finnigan, J.J., 1978. Turbulent flow over a very rough, random surface. Boundary-Layer Meteorol., 15: 109-132.

O'Loughlin, E.M. and Annambhotla, V.S.S., 1969. Flow phenomena near rough boundaries. J. Hydraul. Res., 7: 231-250.

Orlando, A.F., Moffatt, R.J. and Kays, W.M., 1974. Turbulent transport of heat and momentum in a boundary layer subject to suction, deceleration and variable wall temperature. Report No. HMT-17, Thermosciences Division, Dept. of Mech. Eng., Stanford University, Stanford, California, U.S.A.

Raupach, M.R., 1979. Anomalies in flux-gradient relationships over forest. Boundary-Layer Meteorol., 16: 467-486.

Raupach, M.R. and Legg, B.J., 1983. turbulent dispersion from an elevated line source: measurements of wind-concentration moments and budgets. J. Fluid Mech. (in press)

Raupach, M.R. and Thom, A.S., 1981. Turbulence in and above plant canopies. Ann. Rev. Fluid Mech., 13: 97-129.

Raupach, M.R., Thom, A.S. and Edwards, I., 1980. A wind tunnel study of turbulent flow close to regularly arrayed rough surfaces. Boundary-Layer Meteorol., 18: 373-387.

Tennekes, H. and Lumley, J.L., 1972. A first course in turbulence. M.I.T. Press, Cambridge, Mass., U.S.A., 300 pp.

Thom, A.S., 1971. Momentum absorption by vegetation. Q.J.R. Meteorol Soc., 97: 414-428.

Thom, A.S., 1975. Momentum, mass and heat exchange of plant communities. In: J.J. Monteith (Editor), Vegetation and the Atmosphere. Academic Press, London, 1: 57-109.

Townsend, A.A., 1965a. Self-preserving flow inside a turbulent boundary layer. J. Fluid Mech., 22: 773-797.

Townsend, A.A., 1965b. The response of a turbulent boundary layer to abrupt changes in surface conditions. J. Fluid Mech., 22: 799-822.

Yaglom, A.M., 1977. Comments on wind and temperature flux-profile relationships. Boundary-Layer Meteorol., 11: 89-102.